On the Ductility of Cast Al-7 Pct Si-Mg Alloys

MURAT TIRYAKIOĞLU, JOHN CAMPBELL, and NIKOLAOS D. ALEXOPOULOS

The yield strength–elongation relationship in cast Al-7 pct Si-Mg castings has been investigated by analyzing 18 datasets from the literature on premium quality castings. The data representing the elongation for a given yield strength have been found to fall within an envelope, the top limit of which represents the ductility potential of Al-7 pct Si-Mg alloy castings. Analysis of maximum elongation data indicated that secondary arm spacing has no effect on elongation. It has also been determined that the quality index of Drouzy *et al.* does not provide a particularly accurate representation of the trends in maximum ductility data. A new quality index based on those proposed previously by Cáceres and Din *et al.* is proposed. Moreover, using the fracture toughness equation by Hahn and Rosenfield, intrinsic plane strain fracture toughness and intrinsic elongation values have been found to be correlated, indicating the internal consistency of the approach taken in this study. The implications of these results are discussed in the article.

DOI: 10.1007/s11661-008-9762-4

I. INTRODUCTION

ALUMINUM-SILICON cast alloys offer a good combination of mechanical properties and castability, which accounts for their wide use in automotive and aerospace applications. Nevertheless, aluminum castings have been rarely used in critical applications due to concerns about the variability in properties, especially in elongation and fatigue life. This high level of variability is a consequence of structural defects in castings, *i.e.*, pores and oxide bifilms, which degrade mechanical properties; they cause premature fracture in tension[1] and fatigue,[2] resulting in low ductility, tensile strength, and fatigue life.[3] In addition, the presence of major structural defects result in increased variability in properties, as evidenced most notably by lower Weibull moduli.[4,5] Hence, minimization and even elimination of the structural defects is vital for wider use of aluminum castings in structural applications in aerospace and automotive industries.

It might be argued that attributing the high variability of properties only to structural defects such as oxide bifilms (naturally occurring cracks that form *via* a folding-over action) and porosity is an overstatement for Al-Si alloys, because, it has been proposed, the variability in the size of Si particles is a major factor affecting tensile properties.[6] However, there is strong evidence that the Si particles themselves form on folded oxide defects, so that the cracks and decoherence observed to be associated with "unmodified" Si platelets actually also originate from oxide bifilms.[7] In the absence of oxide bifilms, Si has no favored substrate, and so grows at a lower temperature as a "modified" eutectic.[7] Furthermore, there is strong evidence presented in the literature[5,8–13] linking the defect size observed in Al-Si castings to the scatter in tensile and bend strength. Moreover, Finlayson *et al*.[14] found *via* neutron diffraction methods that fracture stress in Si eutectic particles in tension is between 200 and 400 MPa, which is significantly lower than 1200 MPa as suggested previously by Cáceres and Griffiths.[15] Consequently, Finlayson *et al.* suggested that there may be defects in the Si particles leading to their premature fracture in tension, in agreement with the hypothesis that the unmodified Si particles contain oxide bifilms because this was their growth substrate.

Foundry engineers striving to resolve quality concerns in aluminum castings, such as low ductility, often try to change the heat treatment procedure assuming that ductility can be increased mainly by trading off strength. These efforts are usually ineffective unless the root cause of low ductility, *i.e.*, structural defects, is addressed. Hence, when oxide bifilms and porosity are present in castings it is at best inefficient and at worst fruitless to approach the problem from a ductility-strength compromise point of view.

In the quest for improved properties it is helpful for the foundry engineer to have a metric to measure the degree of improvement that they make. The so-called quality indices developed over the years are intended to serve this need. Among the quality factors developed so far, only the ones by Cáceres[16] and Tiryakioğlu *et al*.[17] supply a measure in terms of the ratio of the current to achievable ductility. Both indices determine the achievable quality from the work-hardening characteristics of the specimen. This approach, however, underestimates the true ductility potential of the alloy[18] because structural defects decrease the observed work-hardening rates significantly.[1,19] Therefore, an improved approach is needed to estimate the true ductility potential of cast aluminum alloys. Such an approach is reported in this study.

MURAT TIRYAKIOĞLU, Professor, is with the Department of Engineering, Robert Morris University, Moon Township, PA 15108. Contact e-mail: tiryakioglu@rmu.edu JOHN CAMPBELL, Professor Emeritus, is with Department of Metallurgy and Materials, University of Birmingham, Edgbaston, B15 2TT, United Kingdom. NIKOLAOS D. ALEXOPOULOS, Assistant Professor, is with the Department of Financial and Management Engineering, University of the Aegean, 821 00, Chios, Greece.

Manuscript submitted July 1, 2008.
Article published online February 4, 2009

II. BACKGROUND

Mechanical properties of castings are controlled by the structural defect or concentration of defects that leads to the largest stress concentration. The point of largest stress concentration constitutes the weakest link, which is modeled and assessed by the Weibull distribution.[20] In Al-Si alloy castings, tensile strength, elongation-to-fracture (e_F), and fatigue life are properties related to fracture initiated at the weakest link, and therefore are expected to follow a Weibull distribution as shown in the literature.[2,21,22] Mi *et al.*[23] conducted experiments on Al-4.5 wt pct Cu alloys and found that the Weibull modulus, a measure of reliability, decreases with increasing level of entrainment of surface oxide films. Therefore, there is strong evidence that the mechanical properties of cast aluminum alloys are governed by the size distribution of defects, with the largest defects resulting in premature failure.

In contrast, yield strength (σ_Y) is not expected to follow a Weibull distribution because the weakest link concept does not apply. The material at and around the largest stress concentration yields before the rest of the material, flows plastically, and work hardens, making up, at least partially, for the loss in resistance to deformation. Thus, yield strength should be relatively insensitive to defects, as is commonly observed.

Din *et al.*[24] investigated the change in the tensile properties of A356 and A357 castings with artificial aging time. The authors found linear relationship between elongation (e_F) and yield strength. Based on this result, the authors introduced a quality index Q_{DRC}, which is the yield strength extrapolated to zero elongation, based on the linear relationship between e_F and σ_Y that they observed:

$$Q_{\mathrm{DRC}} = \sigma_Y + k_D e_F \qquad [1]$$

The authors found k_D to be 50 MPa. In an earlier effort, Drouzy *et al.*[25] introduced an empirical equation that defines the relationship between yield strength, tensile strength (S_T), and elongation (for $e_F > 1$ pct):

$$\sigma_Y = S_T - 60\log_{10}(e_F) - 13 \qquad [2]$$

The authors also introduced a quality factor Q_{DJR} for underaged and peak-aged alloys:

$$Q_{\mathrm{DJR}} = S_T + 150\log_{10}(e_F) \qquad [3]$$

Cáceres[16] developed a quality index after explaining the physical basis of Q_{DJR}. Cáceres' quality factor Q_C is a ratio of e_F to elongation expected of the specimen if it were free from structural defects $e_{F(e)}$:

$$Q_C = \frac{e_F}{e_{F(e)}} \qquad [4]$$

Cáceres assumed that cast aluminum alloys follow the well-known Ludwik–Hollomon equation:

$$\sigma = C\varepsilon_p^n \qquad [5]$$

where σ and ε_p are true stress and true plastic strain, respectively, C is the strength coefficient, and n is the strain-hardening exponent. It is well known according to the Considere criterion, that the true plastic strain at the onset of necking (ε_u), *i.e.*, true uniform strain is equal to n, when the material deforms following Eq. [5].[26] In Al-7 pct Si-Mg aluminum aerospace castings, McLellan[27] observed that fracture takes place without almost any necking, and hence, fracture occurs at the nominal uniform elongation value, being approximated as the uniform engineering strain $e_u \approx e_{F(e)} \approx n$.

In the development of a new quality index based on energy absorbed by a specimen prior to fracture, Tiryakioğlu *et al.*[17] estimated $e_{F(\mathrm{int})}$ using work-hardening characteristics, namely, the stage III Kocks–Mecking work-hardening model[28,29] and the Voce equation.[30] However, the authors determined that the late stages of work hardening, where the Considere criterion is met, cannot be estimated accurately from early stages.[18] Hence, if a specimen fractures prematurely due to the presence of structural defects, such as porosity or oxide bifilms, the extrapolation of work-hardening characteristics to higher strains underestimates elongation. This is partially because structural defects reduce the observed work-hardening rates significantly.[1,19] Tiryakioğlu *et al.*[18] also introduced an empirical equation to predict expected elongation as a function of yield strength:

$$e_{F(e)} = \beta_0 \exp(-\beta_1 \sigma_Y) \qquad [6]$$

where β_0 and β_1 are empirical constants.

Nyahumwa *et al.*[31,32] introduced the concept of fatigue life potential and applied it to an Al-7 pct Si-Mg alloy, in which occasionally a specimen would be obtained without a defect, *i.e.*, without the weakest link. Such outliers, then, can be used as a measure of the fatigue life potential or intrinsic fatigue life of the alloy. This approach was applied to elongation data in the present study. Mechanical property data from mostly premium quality (aerospace) castings are analyzed to find trends in *maximum* values. Those data are then analyzed to (1) estimate the ductility potential of cast Al-7 pct Si-Mg alloys, (2) reevaluate the effect of secondary dendrite arm spacing (SDAS) on elongation, (3) reassess the quality indices of Din *et al.*[24] and Drouzy *et al.*,[25] and (4) determine whether there is any relationship between fracture toughness and tensile properties of cast Al7 pct Si-Mg alloys.

III. DATA ANALYSIS AND DISCUSSION

Eighteen datasets for yield strength–elongation-to-fracture were analyzed in this study. Details of the datasets are provided in Table I where n_s represents the number of data. A total of 323 tensile data obtained at room temperature (with strain rates ranging between 10^{-2} and 10^{-3} s^{-1}) were included in this analysis. These datasets cover the composition range of 0.3 to 0.7 wt pct Mg and 6.5 to 7.5 wt pct Si.

The σ_Y-e_F data from the sources shown in Table I are presented in Figure 1, with yield strength plotted in the x-axis because of its relative insensitivity to the presence

Table I. Datasets Used for Yield Strength–Elongation Relationship

Dataset	Alloy	n_s	Reference	Notes
e1	A356	10	9	bars with macropores
e2	D357	34	33	aerospace castings
e3	A357	92	34	aerospace castings
e4	A357	5	35	aerospace and premium castings
e5	A356	4	36	permanent mold and direct chill castings
e6	A356	14	37	cast plates
e7	A356	3	38	hot isostatic pressing (HIP)
e8	A357	42	39	aerospace castings
e9	A357	47	40	continuously cast
e10	D357	8	41	aerospace castings
e11	357	12	42	continuously cast
e12	A357	13	43	aerospace castings
e13	D357	12	12	cast plates, some HIP
e14	A356/A357	6	44	cast plates, HIP
e15	D357	10	45	aerospace castings
e16	A356	3	46,47	rheo-cast, squeeze cast, cast-forged
e17	A356	3	48	continuously cast
e18	A356	5	49	continuously cast

of structural defects for reasons explained previously. In Figure 1, the scatter is mostly vertical due to the varying structural quality of the specimens, as shown previously for cast Al-Si alloys.[9]

Note in Figure 1 that the highest points follow a curvilinear trend. The curve drawn in the figure follows Eq. [6]:

$$e_{F(\text{int})}(\text{pct}) = 42.5\ \exp(-0.0029\sigma_Y) \qquad [7]$$

It is significant that maxima of data taken from different sources indicate such a consistent trend with yield strength. To the authors' knowledge, it is the first time that the ductility potential of cast Al-7 pct Si-Mg alloys is reported, especially with such a large number of data. Equation [7] represents the true strength-ductility compromise in cast Al-7 pct Si-Mg alloys. This ductility potential estimated by Eq. [7] can now be used in lieu of $e_{F(e)}$ in Eq. [4], such that

$$Q_T = \frac{e_F}{42.5\ \exp(-0.0029\sigma_Y)} \qquad [8]$$

A. *The Effect of Microstructure on Ductility*

In Figure 1, the points on or in the vicinity of the maximum ductility curve are assigned numbers. Relevant information about these points, such as SDAS, whether any modification addition was made, average Si particle size (d) and the process by which the specimen was produced are listed in Table II. Note that SDAS values range between 13 and 45 μm and half of the points are from alloys that were not modified with Sr or Na. The fact that these data, obtained from very

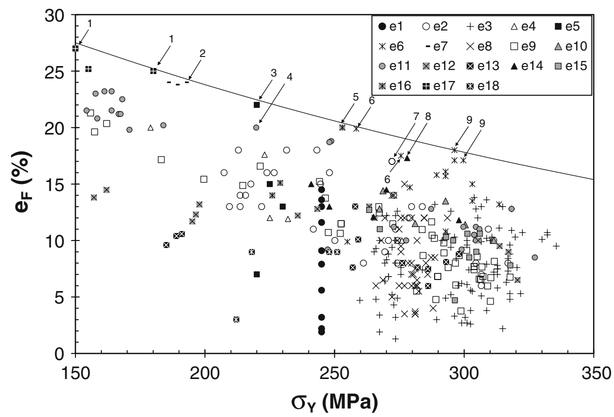

Fig. 1—Yield strength–elongation relationship in Al-7 pct Si-Mg alloy castings.

Table II. Relevant Information about Points Indicated in Figure 1

Data	SDAS (μm)	Modification	d (μm)	Process
1	30*	Sr	2.2*	continuous casting
2	45	Sr	—	sand casting
3	13	Sr	2.5	direct chill casting
4	20	none	—	continuous casting
5	41	none	3.8	cast-forged
6	30	Sr	—	cast plates
7	41	none	—	continuous casting
8	18	Sr	—	cast plates
9	31	none	—	cast plates

*Estimated from micrograph shown in Ref. 49.

different processes and therefore with quite different microstructures, follow the same curve is noteworthy. It is well known[50,51] in the casting literature that elongation increases with decreasing SDAS. For instance, an increase in SDAS from 20 to 45 μm would cause a drop in e_F from (1) 11 to 5 pct in A356, based on the results of Miguelucci;[52] and (2) 10 to 4 pct in A357, based on the results of Wang and Cáceres.[51] Hence, the results of both studies indicate approximately a 60 pct loss in elongation with the increase in SDAS from 20 to 45 μm. This effect has been observed repeatedly in the literature. Although some contribution of SDAS to yield strength as a result of the Hall–Petch effect has been reported,[53] to the authors' knowledge, only a limited number of attempts have been made to explain the strong effect of SDAS on ductility from a micromechanical point of view. For instance, Doglione *et al.*[54] made *in-situ* observations on the damage accumulation to Si particles during a tensile test. They observed that at small SDAS, the numerous and highly-branched interdendritic channels disperse microcracks and consequently delay final fracture. Doglione *et al.* also stated that they did not observe fracture at Si particles followed by microvoid growth and coalescence as the primary failure mechanism, as suggested previously.[55]

Wang and Cáceres[51] developed a different explanation. After approximately 10 pct of Si particles crack during the tensile test, there is a distribution of microcracks in the specimen. Final fracture takes place when these microcracks become unstable, grow, and link with other microcracks. At large SDAS, this instability propagates along the dendritic boundaries, where there is a profusion of damaged Si particles and microcracks, leading to low ductility due to transgranular fracture. At small SDAS, the dendritic boundaries are not continuous. Consequently, microcracks are isolated and their size is reduced. Because the linking of microcracks is now more difficult, tensile ductility is enhanced. However, this explanation is not supported by the *in-situ* observations of Doglione *et al.*[54] and the findings of the present study.

Recently, one of the authors[50,56] suggested that the effect of SDAS can be explained only when bifilms are taken into account. There is a strong relationship between SDAS and local solidification time,[57] and therefore, SDAS is only a measure of how much time is given the bifilms to unfurl during solidification. With long solidification times (large SDAS), bifilms that are compact at the end of mold filling find sufficient time to unfurl under the negative pressure built up during solidification or the diffusion of hydrogen rejected by the solidifying metal to the bifilms. Hence, long solidification times leading to large SDAS result in larger defects which reduce ductility. When bifilms are absent in the area of a casting where a tensile coupon is excised, it can then be expected that SDAS will have only a minor, or even no effect on ductility. The nature of the data indicated in Figure 1 and outlined in Table II provides strong support for this argument. More research is needed to verify this point.

B. *Comparison with the Results of Din et al.*[24]

The e_F-σ_Y data of points indicated in Table II are replotted in Figure 2. Note that the trend in the maximum points can also be expressed by a linear equation. The best fit equation is

$$e_{F(\mathrm{int})} = 36.0 - 0.0647\sigma_Y \qquad [9]$$

The coefficient of determination R^2 for Eq. [9] is 0.95, which is identical to that of Eq. [7]. When Eq. [9] is rearranged to the same form as Eq. [1], k_D is found to be 15.5 MPa, a value significantly less than found by Din *et al.*[24] Equation [4] can now be written as

$$Q_T = \frac{e_F}{36.0 - 0.0647\sigma_Y} \qquad [10]$$

Equation [10] is recommended over Eq. [8] because of its simplicity.

C. *Comparison with Results of Drouzy et al.*[25]

Inserting Eq. [7] into Eq. [2], we obtain

$$\sigma_Y = S_T - 60\log_{10}(42.5\exp(-0.0029\sigma_Y)) - 13 \qquad [11]$$

Because intrinsic uniform elongation is used in Eq. [11], it is reasonable to expect the tensile strength

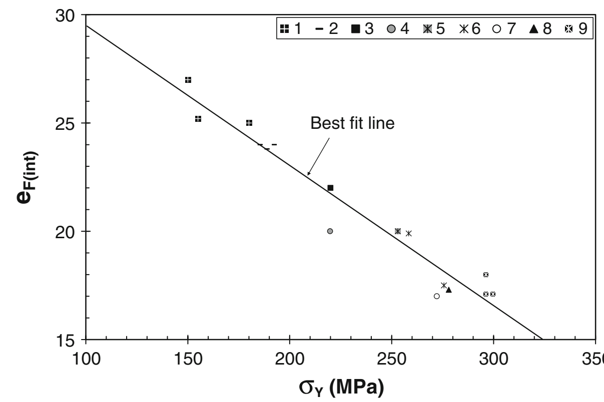

Fig. 2—Yield strength–elongation data for maximum points indicated in Fig. 1 replotted.

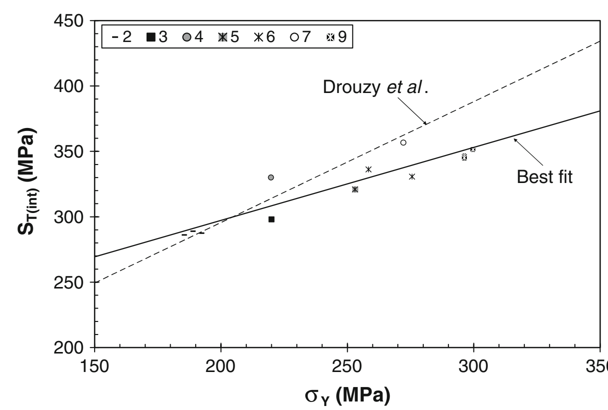

Fig. 3—Yield strength–tensile strength relationship for points indicated in Fig. 1. Equation [12] and best-fit line (Eq. [13]) are also indicated.

to be intrinsic as well. Therefore, after rearranging and canceling logarithmic and exponential functions, intrinsic tensile strength ($S_{T(\mathrm{int})}$)can be written as

$$S_{T(\mathrm{int})} = 110.7 - 0.924\sigma_Y \qquad [12]$$

The tensile strengths of the points as indicated around the curve in Figure 1 are plotted in Figure 3 along with Eq. [12]. (Tensile strengths for points 1 and 8 were unfortunately not quoted in the original references.)

Figure 3 indicates that the relationship developed by Drouzy *et al.*[25] approximates the trend of the data but is clearly not the best fit. The R^2 for Eq. [12] is only 0.11. The best fit line, also shown in Figure 3, has the following equation:

$$S_{T(\mathrm{int})} = 185.7 - 0.558\sigma_Y \qquad [13]$$

with an R^2 of 0.84. Due to the limited number of data, however, the validity of Eq. [12] cannot be ruled out.

Turning our attention to the quality index of Drouzy *et al.*,[25] rearranging Eq. [3] yields

$$S_T = Q_{\mathrm{DJR}} - 150\log_{10}(e_F) \qquad [3a]$$

The logarithm of the elongation for the points indicated in Figure 1 is plotted *vs* tensile strength in Figure 4.

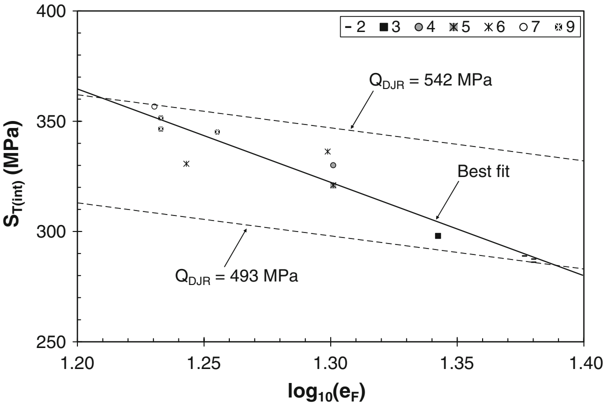

Fig. 4—Elongation *vs* tensile strength of points indicated in Fig. 1. The quality index lines of Drouzy *et al.*[25] as well as the best-fit line are also indicated.

Clearly, the values derived from Eq. [3a] do not fall on a single line as would be expected. The plot of these maximum data might be expected to fall close to a Q_{DJR} value of about 535 MPa, which seems a ceiling value reported in the literature. In fact Q_{DJR} values of 493 to 542 MPa are required to span the scatter; a difference of 49 MPa. This large difference throws serious doubt on the concept of a quality index as defined by Drouzy *et al.*, at least in its present form. The best fit line, indicated in Figure 4, has a slope of −423 MPa and R^2 of 0.92. Therefore, the quality index equation of Drouzy *et al.* (Eq. [3]) should be modified. It is the authors' recommendation that only that Eq. [10] be used to quantify the quality level of Al-7 pct Si-Mg alloy castings.

D. *Relationship between Ductility and Fracture Toughness*

To determine the internal consistency of the approach taken in this study, a possible relationship to fracture toughness potential was also investigated. To determine a possible relationship, the equation introduced by Hahn and Rosenfield,[58] relating fracture toughness K_{Ic} to properties obtained in a tensile test, was used:

$$K_{Ic} = \sqrt{\frac{2\delta E' \sigma_Y \varepsilon_f}{3}} \qquad [14]$$

where δ is the plastic zone width and ε_f is the true fracture strain obtained in a tensile test. The term E' is found by

$$E' = \frac{E}{1 - \upsilon^2} \qquad [15]$$

where E is modulus of elasticity and υ is Poisson's ratio. Hahn and Rosenfield assumed that tensile deformation behavior in the alloys that they investigated follows Eq. [5]. Because strain hardening tends to distribute the strain in a material, δ becomes larger with increasing n. Hahn and Rosenfield, using their experimental data obtained on steels, titanium alloys, and aluminum alloys, showed that

$$\delta = kn^2 \qquad [16]$$

with k = 1 in. (=0.0254 m) in the original work. Inserting Eq. [16] into Eq. [14],

$$K_{Ic} = n\sqrt{\frac{2kE' \sigma_Y \varepsilon_f}{3}} \qquad [17]$$

Hahn and Rosenfield found Eq. [17] to be within 30 pct for 11 different alloys, including some wrought aluminum alloys. Similar results were found by Chen and Knott[59] in 7XXX wrought aluminum alloys.

Based on the observations of McLellan in Al-7 pct Si-Mg alloys, it can be assumed that $\varepsilon_f \approx \varepsilon_u = n$ and, therefore, Eq. [17] can be written as

$$K_{Ic} = n\sqrt{\frac{2kE' \sigma_Y n}{3}} \qquad [18]$$

After rearranging, we obtain

$$n = \left(\frac{3}{2kE'}\frac{K_{Ic}^2}{\sigma_Y}\right)^{\frac{1}{3}} \qquad [19]$$

Equation [19] is almost identical to the one derived previously by Barlat.[60] It should be noted that structural defects reduce the work-hardening rate of cast Al alloys,[1,19] and consequently, n observed in specimens with major structural defects is significantly less than in specimens without major structural defects. Intrinsic plastic uniform elongation, and hence the lower bound for intrinsic total elongation, can then be found by

$$e_{F(\mathrm{int})}(\mathrm{pct}) = 100(\exp(n) - 1) \qquad [20]$$

Combining Eqs. [19] and [20], we obtain

$$e_{F(\mathrm{int})}(\mathrm{pct}) = 100\left(\exp\left(\left(\frac{3}{2kE'}\frac{K_{Ic}^2}{\sigma_Y}\right)^{\frac{1}{3}}\right) - 1\right) \qquad [21]$$

Staley[64] suggested that fracture toughness of aluminum alloys is controlled by extrinsic and intrinsic factors. Extrinsic factors include porosity, oxides, and other inclusions. The intrinsic factors include many fundamental features as the matrix interatomic bonding and crystallographic structure, grain size, *etc*. The true (intrinsic) fracture toughness $K_{Ic(\mathrm{int})}$ cannot be determined unless extrinsic factors are eliminated. Consequently, only intrinsic fracture toughness can be related to the ductility potential of aluminum castings, as expressed by Eq. [21].

One of the authors[61] analyzed K_{Ic}-σ_Y relationship in cast Al-7 pct Si-Mg alloys by using 125 data from 20 datasets reported in the literature. Following the approach of Speidel,[62] the author drew a line just above the maximum points on the K_{Ic}-σ_Y plot, with the line representing the intrinsic plane-strain fracture toughness of cast Al-7 pct Si-Mg alloys:

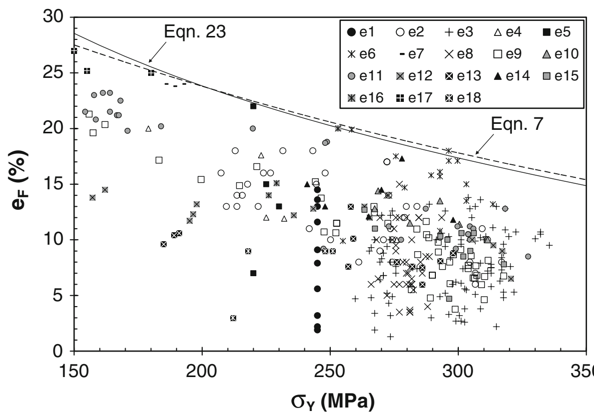

Fig. 5—Fig. 1 replotted to show the fit of Eq. [23] to the data in Table I.

$$K_{Ic(\mathrm{int})} = 50.0 - 0.073\sigma_Y \qquad [22]$$

The linear relationship between plane-strain fracture toughness and yield strength is consistent with the results reported in the literature for various cast[63] and wrought[64–67] aluminum alloys. Combining Eqs. [21] and [22], we obtain

$$e_{F(\mathrm{int})}(\mathrm{pct}) = 100\left(\exp\left(\left(\frac{3}{2kE'}\frac{(50.0-0.073\sigma_Y)^2}{\sigma_Y}\right)^{\frac{1}{3}}\right)-1\right) \qquad [23]$$

The fit obtained by Eq. [23] and the data outlined in Table I are presented in Figure 5, where Eq. [23] was plotted by taking $k = 0.0113$ m, $E = 76$ GPa,[68] and $\upsilon = 0.33$. That the value of k being different from the original value of 0.0254 proposed by Hahn and Rosenfield[58] is consistent with the observations of Chen and Knott[59] in 7XXX wrought aluminum alloys. The curve for $k = 0.0113$ is within 24 pct of the curve that would be obtained with $k = 0.0254$, which is inside the 30 pct error stated by Hahn and Rosenfeld. Clearly, the curve obtained from Eq. [23] agrees with the trend in the maxima of the data in Figure 5 and is very close to the curve of Eq. [7], indicating the internal consistency of the approach taken in this study.

E. *Extrapolations of the Results*

It should be noted that Eqs. [7], [9], and [23] are an estimate of the uniform elongation and should therefore be taken as only a lower bound estimate of the intrinsic total elongation. It was found[69] that powder metallurgy Al-Si-Mg alloys with 10 to 20 pct Si and 0.5 pct Mg, even with a significant amount of aluminum oxide in them, necked and deformed nonuniformly past the point of tensile instability. Consequently, reduction in area (RA) was significantly higher than e_F. For instance, a specimen with 15 pct Si with $\sigma_Y = 358$ MPa, $e_u = 2.3$ pct, and $e_F = 5.5$ pct had a 14 pct RA.

It has been only recently understood[50,70] that the degradation of and variability in the mechanical properties of aluminum castings are related to the defects that are introduced into the molten metal usually as a result of poor handling of the molten metal or poor filling system design. These defects, namely, oxide bifilms, are incorporated into the bulk of the liquid by an entrainment process, in which the surface oxide folds over itself. Unlike steel castings in which the oxide has a significantly lower density than the metal thus floating out quickly and thus leaving the metal clean, the folded aluminum oxide in aluminum has practically neutral buoyancy, so that defects tend to remain in suspension. The layer of air in the folded oxide can grow into a pore or remain as a crack in the solidified alloy.

As a result of the awareness of oxide bifilms raised in the last 15 years, castings continue to be produced to higher quality, with increased melt cleanness and careful filling system design. The elongation-to-fracture, once limited to only 1 or 2 pct, is now steadily increasing and now commonly achieves at least 10 pct in combination with good strength.[7] Figure 1 illustrates that at a yield strength of 320 MPa, an elongation potential of 17 pct should be expected as a result of only uniform plastic elongation. Even greater elongations in practice might be expected from subsequent nonuniform elongation (*i.e.*, necking down to failure). Figure 1 also graphically illustrates the fact that most tensile specimens are currently failing with properties well below these predictions, indicating a widespread density of serious defects in most cast aluminum alloys.

Without structural defects, the matrix can be expected to behave as a perfectly plastic material and should continue to stretch plastically, necking down significantly. In cast Al-7 pct Si-Mg alloys, the Si eutectic particles do not deform plastically. Thus, RA should be reduced by the area fraction (*i.e.*, volume fraction) of the Si, which is 10 to 15 pct. Thus the total predicted ductility for defect-free alloy can be speculated to be around 85 pct RA. This level of ductility is often seen in clean metallic systems such as many steels. Ultimately, elongations in Al alloys, typical of steels in the range 30 to 50 pct, are to be expected if metal cleanness continues to be enhanced.

IV. CONCLUSIONS

1. The analysis of the 18 yield strength–elongation bivariate datasets showed that there is a strong relationship between the maximum elongation values and yield strength.
2. The curve fitted to the maximum data represents the true strength-ductility compromise in cast Al-7 pct Si-Mg alloys.
3. The analysis of the maximum elongation data showed that SDAS has no effect on the elongation, supporting the hypothesis that SDAS is only a measure of time given to bifilms to unfurl during solidification. In the absence of bifilms, SDAS has no significant effect. More research is needed in this area.

4. The analysis of maximum elongation data also indicated that the valuable quality index concept introduced and developed by Drouzy *et al.*[25] unfortunately did not represent the true quality of the castings adequately. It is proposed that a new quality index based on the quality indices proposed by Cáceres[16] and Din *et al.*[24] and the observed ductility potential of cast Al-7 pct Si-Mg alloys be used instead. The new quality factor is calculated as

$$Q_T = \frac{e_F}{36.0 - 0.0647\sigma_Y}$$

5. The fracture toughness equation developed by Hahn and Rosenfield[58] has been modified to express the relationship between yield strength, intrinsic fracture toughness, and intrinsic ductility. The modified equation followed the trends of the maxima of the datasets, indicating the internal consistency of the approach taken in this study.
6. The data of the vast majority of the quality of Al-7 pct Si-Mg specimens indicate that mechanical performance falls well below these predictions, implying evidence of a population of defects.
7. An upper bound of 17 pct uniform elongation is predicted at 320 MPa yield strength for Al-7 pct Si-Mg alloys in (uniform) plastic extension. Even higher elongations, allowing a further regime of extension in which necking to failure may occur, seem likely to be achievable with adequate cleanness.

REFERENCES

1. M. Tiryakioğlu, J. Campbell, and J.T. Staley: *Scripta Mater.*, 2003, vol. 49, pp. 873–78.
2. C. Nyahumwa, N.R. Green, and J. Campbell: *Metall. Mater. Trans. A.*, 2001, vol. 32A, pp. 349–58.
3. J.T. Staley, Jr., M. Tiryakioğlu, and J. Campbell: *Mater. Sci. Eng. A*, 2007, vol. A465, pp. 136–45.
4. N.R. Green and J. Campbell: *Mater. Sci. Eng. A*, 1993, vol. A173, pp. 261–66.
5. X. Dai, X. Yang, J. Campbell, and J. Wood: *Mater. Sci. Eng. A*, 2003, vol. A354, pp. 315–25.
6. M. Tiryakioğlu: *Mater. Sci. Eng. A*, 2006, vol. A427, pp. 154–59.
7. J. Campbell: *The Bifilm Concept: Prospects of Defect-Free Castings*, World Foundry Congress, Chennai, India, 2008.
8. X. Yang, X. Huang, X. Dai, J. Campbell, and R.J. Grant: *Mater. Sci. Technol.*, 2006, vol. 22, pp. 561–70.
9. M.K. Surappa, E. Blank, and J.C. Jaquet: *Scripta Metall.*, 1986, vol. 20, pp. 1281–86.
10. L. Liu and F.H. Samuel: *J. Mater. Sci.*, 1998, vol. 33, pp. 2269–81.
11. G.E. Byczynski and J. Campbell: in *Advances in Aluminum Casting Technology II*, M. Tiryakioğlu and J. Campbell, eds., ASM INTERNATIONAL, Materials Park, OH, 2002, pp. 65–74.
12. J.A. Francis and G.M. Delphine Cantin: *Mater. Sci. Eng. A*, 2005, vol. A407, pp. 322–29.
13. Z. Ma, A.M. Samuel, F.H. Samuel, H.W. Doty, and S. Valtierra: *Mater. Sci. Eng. A*, 2008, vol. A490, pp. 36–51.
14. T.R. Finlayson, J.R. Griffiths, D.M. Viano, M.E. Fitzpatrick, E.C. Oliver, and Q.G. Wang: *Shape Casting: 2nd Int. Symp.*, P.N. Crepeau, M. Tiryakioğlu, and J. Campbell, eds., TMS, Warrendale, PA, 2007, pp. 127–34.
15. C.H. Cáceres and J.R. Griffiths: *Acta Mater.*, 1996, vol. 44, pp. 25–33.
16. C.H. Cáceres: *Int. J. Cast Met. Res.*, 1998, vol. 10, pp. 293–99.
17. M. Tiryakioğlu, J.T. Staley, and J. Campbell: *Mater. Sci. Eng. A*, 2004, vol. A368, pp. 231–38.
18. M. Tiryakioğlu, J. Campbell, and J.T. Staley: *Mater. Sci. Eng. A*, 2004, vol. A368, pp. 205–11.
19. M. Tiryakioğlu, J.T. Staley, Jr., and J. Campbell: *Mater. Sci. Eng. A*, 2008, vol. A487, pp. 383–87.
20. W. Weibull: *J. Appl. Mech.*, 1951, vol. 8, pp. 293–97.
21. N.R. Green and J. Campbell: *Mater. Sci. Eng. A*, 1993, vol. A137, pp. 261–66.
22. H. Zahedi, M. Emamy, A. Razaghian, M. Mahta, J. Campbell, and M. Tiryakioğlu: *Metall. Mater. Trans. A.*, 2007, vol. 38A, pp. 659–70.
23. J. Mi, R. Harding, and J. Campbell: *Metall. Mater. Trans. A*, 2004, vol. 35A, pp. 2893–2902.
24. T. Din, A.K.M.B. Rashid, and J. Campbell: *Mater. Sci. Technol.*, 1996, vol. 12, pp. 269–73.
25. M. Drouzy, S. Jacob, and M. Richard: *AFS Int. Cast Met. J.*, 1980, vol. 5, pp. 43–50.
26. G. Dieter: *Mechanical Metallurgy*, McGraw-Hill, New York, NY, 1988, pp. 340–43.
27. D.L. McLellan: *J. Test. Eval.*, 1980, vol. 8, pp. 170–76.
28. U.F. Kocks: *J. Eng. Mater. Technol.*, 1976, vol. 98, pp. 76–85.
29. H. Mecking and U.F. Kocks: *Acta Metall.*, 1981, vol. 29, pp. 1865–75.
30. E. Voce: *Metallurgia*, 1955, vol. 51, pp. 219–26.
31. C. Nyahumwa, N.R. Green, and J. Campbell: in *Advances in Aluminum Casting Technology*, M. Tiryakioğlu and J. Campbell, eds., ASM INTERNATIONAL, Materials Park, OH, 1998, pp. 225–33.
32. C. Nyahumwa, N.R. Green, and J. Campbell: *J. Mech. Behav. Mater.*, 1998, vol. 9, pp. 227–35.
33. K.J. Oswalt and A. Maloit: *AFS Trans.*, 1990, vol. 98, pp. 865–77.
34. D.L. McLellan and M.M. Tuttle: *Manufacturing Methodology Improvement for Aluminum Casting Ductility,* AFWAL-TR-82-4135, The Boeing Company, Seattle, WA, Dec. 1982.
35. J.G. Kaufman and E.L. Rooy: *Aluminum Alloy Castings: Properties, Processes and Applications*, ASM INTERNATIONAL, Materials Park, OH, 2004, pp. 69–122.
36. S. Kumai, T. Tanaka, H. Zhu, and A. Sato: *Mater. Trans.*, 2004, vol. 45, pp. 1706–13.
37. K.A. Yoshida: M.Sc. Thesis, University of Texas–El Paso, El Paso, TX, 1995.
38. S. Mashl: Bodycote Corporation, Andover, MA, private communication, 2008.
39. J.D. Gruner: Northrop Internal Report No. NOR 94-026, Northrop Corporation, Hawthrone, CA, 1994.
40. M. Tiryakioğlu and N.D. Alexopoulos: *Metall. Mater. Trans. A*, vol. 39A, pp. 2772–80.
41. M.W. Ozelton, S.J. Mocarski, and P.G. Porter: *Durability and Damage Tolerance of Aluminum Castings*, WL-TR-91-4111, Northrop Corporation, Hawthrone, CA, 1991.
42. J.T. Staley: Alcoa Progress Report No. 13-HP160, Alcoa, Alcoa Center, PA, 1966.
43. K.J. Oswalt and Y. Lii: *Manufacturing Methods for Process Effects on Aluminum Casting Allowables*, AFWAL-TR-84-4117, Northrop Corporation, Hawthrone, CA, 1985.
44. Q.G. Wang and C.H. Cáceres: *Proc. Int. Conf. on Solidification of Light Alloys*, Gold Cost, Queensland, Aug. 30–31, 1995, pp. 33–37.
45. T.L. Reinhart: Presented at *Aeromat*, Anaheim, CA, 1994.
46. Y.N. Kwon, K. Lee, and S. Lee: *Key Eng. Mater.*, 2007, vols. 345–346, pp. 633–36.
47. K.H. Lee, Y.N. Kwon, and S.H. Lee: *J. Kor. Inst. Met. Mater.*, 2007, vol. 45, pp. 18–29.
48. P.R. Austen and H.M. Williamson: *J. Aust. Inst. Met.*, 1975, vol. 20, pp. 39–43.
49. D.S. Saunders, B.A. Parker, and J.R. Griffiths: *J. Aust. Inst. Met.*, 1975, vol. 20, pp. 33–38.
50. J. Campbell: *Castings,* 2nd ed., Elsevier, New York, NY, 2003, pp. 274–75.
51. Q.G. Wang and C.H. Cáceres: *Mater. Sci. Eng. A*, 1998, vol. A241, pp. 72–82.
52. E.W. Miguelucci: *AFS Trans.*, 1985, vol. 93, pp. 913–16.
53. M. Wierzbinska and J. Sieniawski: *Int. J. Cast. Met. Res.*, 2004, vol. 17, pp. 267–70.

54. R. Doglione, J.L. Douziech, C. Berdin, and D. Francois: *Mater. Sci. Forum.*, 1996, vols. 217–222, pp. 1435–40.
55. C. Meyers and J.S. Chou: *AFS Trans.*, 1991, vol. 99, pp. 165–73.
56. J. Campbell: *Metall. Mater. Trans. B.*, 2006, vol. 37B, pp. 857–63.
57. M.C. Flemings: *Solidification Processing*, McGraw-Hill, New York, NY, 1974, pp. 146–54.
58. G.T. Hahn and A.R. Rosenfield: in *Applications Related Phenomena in Titanium Alloys*, ASTM Special Technical Publication No. 432, ASTM, Philadelphia, PA, 1968, pp. 5–32.
59. C.Q. Chen and J.F. Knott: *Met. Sci.*, 1981, vol. 15, pp. 357–64.
60. F. Barlat: Alcoa Internal Report No. 04-115, Alcoa, Alcoa Center, PA, 2004.
61. M. Tiryakioğlu: *Mater. Sci. Eng. A*, 2007, vol. A497, pp. 512–14.
62. M.O. Speidel: *6th Eur. Non-Ferrous Metals Industry Colloquium of the CAEF*, 1982, pp. 65–78.
63. G.D. Scott, B.A. Cheney, and D.A. Granger: in *Technology for Premium Quality Castings*, E. Dunn and D.R. Durham, eds., TMS, Warrandale, PA, 1988, pp. 123–49.
64. J.T. Staley: in *Properties Related to Fracture Toughness*, ASTM STP. 605, 1976, pp. 71–96.
65. K.V. Jata and E.A. Starke, Jr.: *Metall. Trans. A.*, 1986, vol. 17A, pp. 1011–26.
66. S. Kang and N.J. Grant: *Mater. Sci. Eng.*, 1985, vol. 72, pp. 155–62.
67. N. Kamp, I. Sinclair, and M.J. Starink: *Metall. Mater. Trans A.*, 2002, vol. 33A, pp. 1125–36.
68. D.J. Lloyd: *Int. Mater. Rev.*, 1994, vol. 39, pp. 1–23.
69. W.H. Hunt, Jr.: Ph.D. Dissertation, Carnegie Mellon University, Pittsburgh, PA, 1992.
70. J. Campbell: *Mater. Sci. Technol.*, 2006, vol. 22, pp. 127–45 and 999–1008.